Molecular biological mechanism of BBB modulation using low intensity focused ultrasound in vivo rat models

Kyung Won Chang

Department of Medicine

The Graduate School, Yonsei University

Molecular biological mechanism of BBB modulation using low intensity focused ultrasound in vivo rat models

Kyung Won Chang

Department of Medicine

The Graduate School, Yonsei University

Molecular biological mechanism of BBB modulation using low intensity focused ultrasound in vivo rat models

Directed by Professor Won Seok Chang

The Doctoral Dissertation
submitted to the Department of Medicine,
the Graduate School of Yonsei University
in partial fulfillment of the requirements for the degree
of Doctor of Philosophy in Medicine

Kyung Won Chang

December 2021

This certifies that the Doctoral Dissertation of Kyung Won Chang is approved.

Thesis Supervisor : Won Seok Chang

Thesis Committee Member#1 : Jong Eun Lee

Thesis Committee Member#2 : Sung-Rae Cho

Thesis Committee Member#3: Bong Soo Kim

Thesis Committee Member#4: Ji Hee Kim

The Graduate School
Yonsei University

December 2021

ACKNOWLEDGEMENTS

First of all, I would like to express my deep and sincere gratitude to my research supervisor professor Won Seok Chang. He gave me this wonderful opportunity to do the research and provided invaluable guidance throughout this research. I also want to thank all the researchers in Prof. Chang's laboratory for helping me complete this research.

I am always thankful to my parents for all their love and caring they gave for me. I am very much thankful to my lovely wife and my son which is about to be born. Our family's love, understanding, and continuous support encouraged me to complete this research work

<TABLE OF CONTENTS>

<LIST OF FIGURES, LIST OF TABLES>

LIST OF FIGURES

LIST OF TABLES

ABSTRACT

Molecular biological mechanism of BBB modulation using low intensity focused ultrasound in vivo rat models

Kyung Won Chang

Department of Medicine
The Graduate School, Yonsei University

(Directed by Professor Won Seok Chang)

Low-intensity focused ultrasound is an effective method for inducing blood-brain barrier (BBB) opening, but its underlying mechanisms remain unknown. This study investigated the molecular mechanisms of BBB opening induced by low-intensity focused ultrasound. Rats were sacrificed at different timepoints (1, 4, 24, and 48 h) after receiving focused ultrasound sonication (FUS). Immunohistochemistry and western blot were performed to assess levels of tight junction proteins (occludin and ZO-1) and transcytosis proteins (major facilitator superfamily domain-containing 2a [MFSD2a] and caveolin-1). Levels of ZO-1 and occludin were most prominently decreased at 1 h after FUS at the timepoint when the transient BBB opening was most prominent based on Evans blue extravasation. Caveolae formed predominantly at 4 h post-sonication. MFSD2a levels were lower after FUS. At 4 h post-sonication, MFSD2a levels showed the greatest decrease whereas caveolin-1 levels showed the greatest increase. In conclusion, our results highlight a temporal window between transcytosis and tight junction mechanisms. Therefore, the timepoint of injections should be taken into consideration depending on specific characteristics of the drug when delivering a drug following ultrasound-induced BBB opening.

Key words: blood-brain-barrier, mr-guided focused ultrasound.

Molecular biological mechanism of BBB modulation using low intensity focused ultrasound in vivo rat models

Kyung Won Chang

Department of Medicine
The Graduate School, Yonsei University

(Directed by Professor Won Seok Chang)

I. INTRODUCTION

The blood-brain barrier (BBB) is a specialized structure in the brain that consists of brain-specific endothelial cells, a basement membrane, pericytes, and astrocytic end feet[1,2]. The BBB forms a boundary that separates the circulation of blood and cerebrospinal fluid in the central nervous system (CNS). The BBB exists along all CNS capillaries and consists of a closed membrane around CNS capillaries; this membrane does not exist in extra-cranial circulation[3]. Brain endothelial cells are linked via tight junctions[4], which comprise tight junction proteins including claudin, occludin, and junctional adhesion molecule (JAM), as well as scaffolding proteins such as ZO. Scaffolding proteins bind to tight junction proteins to establish strong structural adhesion[5]. The presence of tight junctions limits paracellular transportation. Further, the lack of fenestrations and transport vesicles limits transcellular transportation and prevents penetration by large molecules[6]. Consequently, this prevents the spread of large molecules or microorganisms into the cerebrospinal fluid[7]. Therefore, the BBB is critical for maintaining homeostasis and protecting the CNS from toxic materials[3,4,7]. Nevertheless, the presence of the BBB also limits the transportation of drugs and poses a significant obstacle to the delivery of pharmaceutical treatments for brain diseases[3,4,7]

Transport of molecules occurs via several pathways. Small hydrophobic molecules necessary for respiration such as H_2O, CO_2, and O_2 spread by passive diffusion[8]. Specific transporter systems exist to enable the controlled transport of necessary peptides and proteins[6,8]. Cells in the BBB are responsible for transporting metabolites such as glucose across certain protein barriers[6,7]. The BBB also contains ion transporters that regulate Na^+, K^+, and Cl^- ion concentrations across the barrier. In addition, the BBB expresses receptors for transport via caveolae-dependent endocytosis, transcytosis, and active exocytosis mechanisms to ensure that any toxic molecules that pass through the BBB are extruded[6-8].

Methods for facilitating transport pathways to enhance drug delivery and clearance of neurotoxic materials are an active field of research[3,6,7,9]. Various drug delivery methods are based on pathological disruptions in the BBB[9,10]. Nevertheless, it remains unclear whether pathologic BBB disruption is a cause or consequence of disease[10,11]. Investigating the mechanisms of BBB disruption may afford novel methods to overcome the low permeability of the BBB[9]. Several techniques are used to bypass the BBB[7]. Invasive techniques such as direct injections can be employed, but the need for surgical interventions is associated with substantial risks and complications. Further, the infiltration of agents into the parenchyma may be limited by diffusion[7]. Therefore, non-invasive techniques are actively being developed[6,7,9]. Techniques such as carrier proteins, pharmacological modifications, virus-mediated delivery, exosome-mediated delivery, intranasal delivery, and BBB permeability modulation such as osmotic agents or focused ultrasound are currently employed[7].

Low-intensity focused ultrasound (FUS) is used to transiently and reversibly open the BBB in target regions[12-14]. Hynynen and colleagues modified the low-intensity FUS method to produce safe and reproducible BBB opening, and microbubbles are used to facilitate FUS-induced BBB

opening[12,15,16]. Extensive research on BBB opening for drug delivery is underway[6,7,17]. Indeed, transient BBB disruption in target brain regions can facilitate the delivery of large pharmacologic agents into the parenchyma[6]. Nevertheless, the mechanisms by which FUS induces BBB opening are unclear[7,18-20]. Several theories have been proposed, including paracellular passage via widened tight junctions[18], transcytosis using cellular vesicles such as carrier- or receptor-mediated transport[18,20], endocytosis[20,21], and cytoplasmic channels in the endothelium[22]. Microbubble oscillation causes stable, inertial cavitation of endothelial cells and likely underpins BBB opening[23-25]. Further, vascular endothelial cells respond dynamically to sheer stress[17,18,26]. Mechanical stresses generated by microbubbles may stimulate mechanosensitive ion channels in endothelial cells[17].

Elucidating the mechanisms of FUS-induced BBB opening will enable the development of methods to maximize BBB opening[6]. This will facilitate drug delivery for treating CNS diseases as well as neurodegenerative disorders, given the potential for promoting the clearance of neurotoxic proteins or particles in neurodegenerative disorders such as Alzheimer's disease and Parkinson's disease[11,27]. Therefore, this study aimed to investigate the molecular mechanisms underpinning BBB opening induced by low-intensity FUS in order to improve the efficiency of BBB opening. To this end, this study reviewed candidate proteins identified in *in vitro* studies and employed an *in vivo* rat model to assess tight junction proteins and proteins involved in the transcellular transcytosis pathway such as Major facilitator superfamily domain-containing 2a (MFSD2a) and caveolin-1.

II. MATERIALS AND METHODS

1. Animals

All animal experiments were performed according to the Guide for the Care and Use of Laboratory Animals of the National Institutes of Health and were approved by the Institutional Animal Care and Use Committee of Yonsei University, Korea (IACUC number: 2019-0208). Animals were housed in groups of three per cage under a 12-h light/dark cycle and controlled humidity (55 ± 5%) and temperature (23 ± 2℃). Food and water were available *ad libitum*. Male Sprague-Dawley rats (n=65, weighing 240-270 g) were randomly divided into five groups, comprising a control group and four FUS sonication groups. The control group (n=13) did not receive any treatment. FUS groups were sacrificed at 1, 4, 24, and 48 h after FUS sonication.

2. FUS sonication

FUS sonication parameters were selected based on a previous study[28], using a 515 kHz single-element spherically focused transducer (H-107MR; Sonic Concept Inc., Bothell, WA, USA; focal depth: 51.7 mm; radius of curvature: 63.2 mm), waveform generator (33220A, Agilent, Palo Alto, CA, USA), and radio frequency power amplifier (240L, ENI Inc., Rochester, NY, USA). Electrical impedance of the transducer was matched to the output impedance of the amplifier (50 Ω) with an external matching network (Sonic Concept Inc., Bothell, WA, USA). A cone filled with distilled and degassed water was mounted onto the transducer assembly. A needle-type hydrophone (HNA-0400; Onda, Sunnyvale, CA, USA) was used for transducer calibration to measure the acoustic beam profile in the tank filled with degassed water. The sonication parameters were: 0.2 MPa average peak-negative pressure and 10-ms burst duration at a 1-Hz pulse-repetition frequency for a total duration of 120 s.

Animals were deeply anesthetized with a mixture of ketamine (75 mg/kg),

acepromazine (0.75 mg/kg), and xylazine (4 mg/kg) and placed in a stereotaxic frame using ear and nose bars. After the scalp was incised, ultrasound transmission gel (ProGel-Dayo Medical Co., Seoul, South Korea) was applied to cover the area between the animal's skull and cone tip to maximize the transmission efficiency of the ultrasound. The FUS target region was the right hippocampal area (AP: −3.5 mm; ML: +2.5 mm from bregma). Definity microbubbles (mean diameter range: 1.1–3.3 μm; Lantheus Medical Imaging, North Billerica, MA, USA) diluted in saline were injected intravenously into the tail vein 10 s prior to ultrasound sonication. Evans blue dye (2%, 100 mg/kg) was injected intravenously at each time point post-sonication in the rats (n = 2 each group), which were sacrificed 30 min later to examine BBB permeability.

3. Magnetic resonance imaging

Magnetic resonance imaging (MRI) was performed with a Bruker 9.4 T 20-cm bore MRI system (Biospec 94/20 USR; Bruker, Ettlingen, Germany) and a rat head coil 1 h after ultrasound sonication. A gadolinium-based contrast agent, dotarem (meglumine gadoterate; Guerbet, Villepinte, France; 0.2 mL/kg), was injected into the tail vein. Contrast-enhanced T1-weighted images were obtained to confirm FUS-induced BBB opening (Fig. 1a). T2-weighted images were obtained to confirm edema with FUS (Fig. 1b). T1-weighted images were obtained without the use of dotarem contrast (Fig. 1c). MRI sequences are detailed in Table 1.

4. Hematoxylin & eosin staining

Hematoxylin (Vector Labs, Burlingame, CA, USA) & eosin (Sigma-Aldrich, St. Louis, MO, USA) (H&E) staining was performed (n=2 for each group) to determine brain hemorrhage and damage. Brains were embedded in paraffin-wax, sectioned into 4-μm sections, and stained with

H&E. Tissues were observed using an optic microscope (BX51; Olympus, Tokyo, Japan).

5. Transmission electron microscopy analysis

Transmission electron microscopy (TEM) was performed to quantify the number of caveolae. Hippocampi were extracted from rats (n = 2 per group). Tissues were fixed for 12 h in 2% glutaraldehyde/paraformaldehyde in 0.1 M phosphate buffer (pH 7.4) and washed in 0.1 M phosphate buffer. Subsequently, tissues were post-fixed with 1% OsO_4 dissolved in 0.1 M PB for 2 h, serially dehydrated in an ascending gradient of ethanol (50−100%), and incubated in propylene oxide. Specimens were embedded using Poly/Bed 812 kit (Polysciences, Warrington, PA, USA) and subjected to fresh resin embedding and polymerization in an electron microscope oven (TD-700, DOSAKA, Japan) for 24 h at 65℃. Sections of 70-nm thickness were cut using LEICA EM UC-7 (Leica Microsystems, Austria) with a diamond knife (Diatome®, Hatfield, PA, USA), transferred to copper and nickel grids, and observed using TEM (JEM-1011, JEOL, Japan)

6. Histological analysis

Animals were anesthetized (via ketamine (75mg/kg) - xylazine(4mg/kg) mixture) and perfused with 0.9% saline and 4% paraformaldehyde at 1 h, 4 h, 24 h, and 48 h after FUS sonication. Brains were extracted and post-fixed in 4% paraformaldehyde (Duksan, Seoul, Korea) for 3 days at 4℃. After postfixation, the brains were transferred to 30% sucrose (Duksan, Seoul, South Korea) for 3 days at 4℃. The brains were sectioned into 30-㎛ sections using a cryostat (Leica Biosystems, Wetzlar, Germany) and stored in cryoprotectant solution consisting of 0.1 M phosphate buffer (pH 7.2), 30% sucrose, 1% polyvinylpyrrolidone (Sigma-Aldrich, St. Louis, MO, USA), and 30% ethylene glycol (Thermo Fisher Scientific, Rockford, IL, USA) at −20℃.

7. Western blot analysis

Animals (n=6 for each group) were anesthetized (ketamine – xylazine mixture) and rapidly decapitated at 1 h, 4 h, 24 h, and 48 h after FUS sonication. Brains were removed and hippocampi were dissected with fine forceps using a 1-mm coronal brain slicer matrix. For protein extraction, tissues were homogenized with lysis buffer (PRO-PREP, Catalog no. 17081, iNtRON Biotechnology, Seongnam, Korea) and centrifuged for 20 min at 12,000 rpm. The supernatant was measured using a bicinchoninic acid protein assay reagent kit (Pierce, Rockford, IL, USA). Proteins were separated using 12% sodium dodecyl sulfate polyacrylamide gels and transferred onto polyvinylidene fluoride membranes. The membranes were blocked with a buffer consisting of 5% nonfat dry milk in Tris-buffered saline with Tween (TBST, Sigma-Aldrich, St. Louis, MO, USA) for 1 h at room temperature. After blocking, the membranes were incubated with anti-MFSD2a (ab177881; 1:1000; Abcam, Cambridge, UK), anti-caveolin-1 (ab2910; 1:1000; Abcam, Cambridge, UK), and anti-β-actin (1:20000; Sigma-Aldrich, , St. Louis, MO, USA) primary antibodies at 4℃ overnight. The membranes were incubated with goat anti-rabbit IgG(H+L)-HRP (1:2000 for MFSD2a and caveolin-1; GenDEPOT, Katy, TX, USA) and goat anti-mouse IgG(H+L)-HRP (1:20000 for β-actin; GenDEPOT, Katy, TX, USA) secondary antibodies for 2 h (room temperature). Proteins were detected using enhanced chemiluminescence solution (WEST-Queen, western blot detection kit, iNtRON Biotechnology, Seongnam, Korea). Signals were obtained using LAS 4000 mini (GE Healthcare Life Sciences, Chicago, IL, USA). Band signals were assessed using an analysis system (Multi Gauge version 3.0, Fujifilm, Tokyo, Japan).

8. Immunofluorescence staining

To detect caveolin-1 and endothelial cells, brain sections (n=1 each group)

were blocked with 5% normal goat serum (Vector Labs, Burlingame, CA, USA) and incubated with primary antibodies for markers of caveolae (Caveolin-1; ab2910; 1:200; Abcam, Cambridge, UK) and endothelial cells (RECA-1; MCA970R; 1:150; Serotec, Oxford, UK) at 4℃ overnight. The sections were then incubated with Alexa Fluor 488 (AF488; A11008; 1:300; Thermo Fisher Scientific, USA) and Alexa Fluor 594 (AF594; A11005; 1:300; Thermo Fisher Scientific, USA) secondary antibodies at room temperature for 2 h. Sections were mounted with DAPI mounting medium (Vector labs, Burlingame, CA, USA). Fluorescent images were obtained using a Zeiss Axio Imager M2 microscope (Carl Zeiss, Oberkochen, Germany).

9. Statistical analysis

Data are expressed as mean ± standard error of the mean (SEM). Data were analyzed using parametric analysis (unpaired t-test). GraphPad Prism 7 software (GraphPad Software, Inc., San Diego, CA, USA) was used for statistical analyses. $p < 0.05$ was considered statistically significant.

Table 1. Sequence of MRI.

	T1-weighted / Gadolinium-enhanced T1-weighted images	**T2-weighted images**
Echo	1	1
TR (ms)	500	2500
TE (ms)	8.1	33
FA (deg)	180	180
NEX	5	2
FOV (cm)	4.0	4.0
Matrix	256 x 256	256 x 256

(TR: repetition time, TE: time to echo, FA: fractional anisotropy, NEX: number of excitations, FOV: field of view)

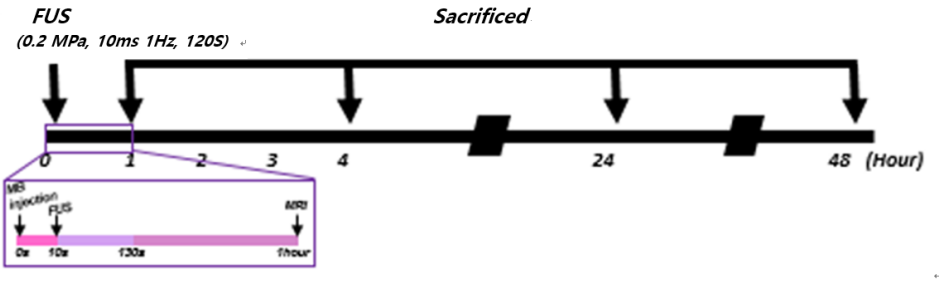

Figure 1. Schematic of the experimental procedure and FUS system. Timeline of the focused ultrasound (FUS) experiment for comparison 1h, 4h, 24h, 48h after sonication.

III. RESULTS

1. Confirmation of safety and reproducibility

To confirm safety and reproducibility of the protocol, MR imaging and H&E staining were performed (Figure 2). MRI was performed 1 h after sonication to confirm signal changes in the right hippocampal area. The targeted area showed T1 gadolinium enhancement which indicates extravasation of contrast agents that suggests successful BBB opening. Minimal FUS-induced edema was observed which can be detected as high signal intensity in T2. No hemorrhage was observed in H&E staining. These findings supported the safety and reproducibility of the protocol in experimental and control groups. TEM revealed tight junction widening in the experimental group compared to that in the control group (Figure 3).

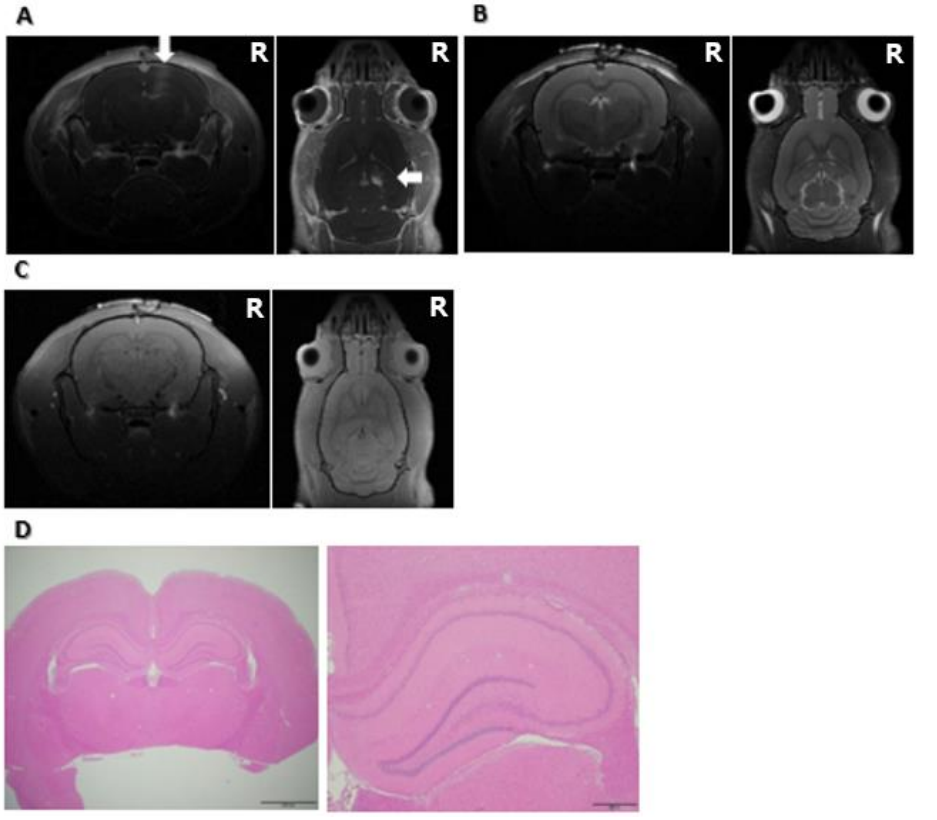

Figure 2. MR imaging and H & E staining **A**: Confirmed FUS-mediated blood-brain barrier (BBB) opening with MRI. Gadolinium-enhanced T1-weighted images show contrast enhancement. **B**: Confirmed FUS with T2-weighted MRI showing minimal edema **C**: Confirmed with T1-weighted MRI **D**: H & E staining for the identification of tissue safety

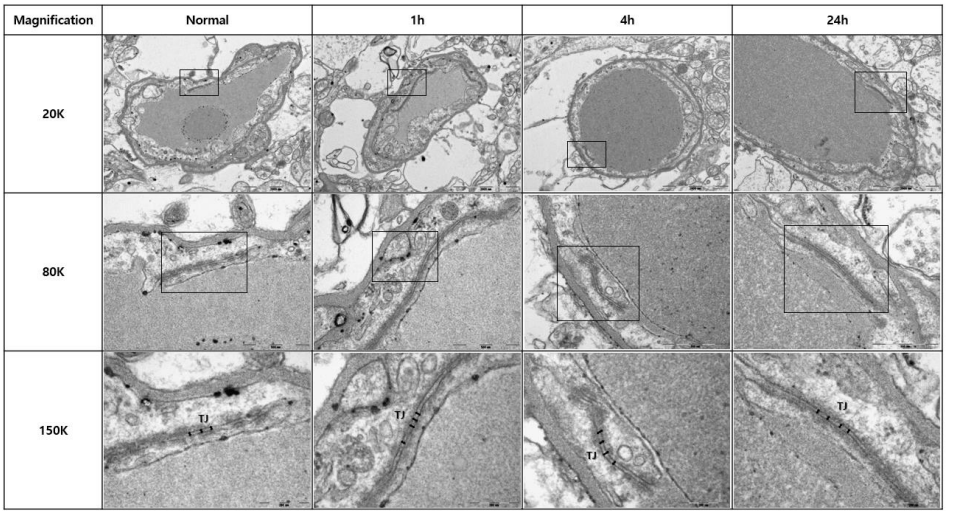

Figure 3. TEM analysis of widened Tight junction after FUS sonication. (Box indicates magnification area, Bidirectional arrow indicates tight junction, TJ : tight junction, Scale bar 20K : 2000nm , 80K : 500nm, 150K : 200nm)

2. Changes in levels of tight junction proteins ZO-1 and occludin after FUS

Western blot analysis was performed to evaluate the levels of tight junction proteins. Levels of the tight junction proteins ZO-1 and occludin were lowest at 1 h after FUS, and gradually recovered to pre-sonication levels in 48 h post sonication. Evans Blue was used to visualize changes in BBB permeability. Evans blue extravasation in brain tissue was observed following FUS. No extravasation was noted in the control group. The most prominent extravasation was observed 1 h post-sonication. Extravasation gradually decreased over time and reached the lowest levels at 24 h after FUS, indicating recovery of BBB opening (Figure 4).

3. Formation of caveolae after FUS

The number of caveolae after exposure FUS was quantified using TEM. Compared to that in the control group, the number of caveolae started to increase at the 1-h timepoint after FUS. Caveolae formed predominantly at the 4-h timepoint FUS. Caveolae were typically observed in endocytosis and transcytosis, suggesting that the greatest transcellular pathway activity and BBB opening occurred at 4 h after sonication (Figure 5).

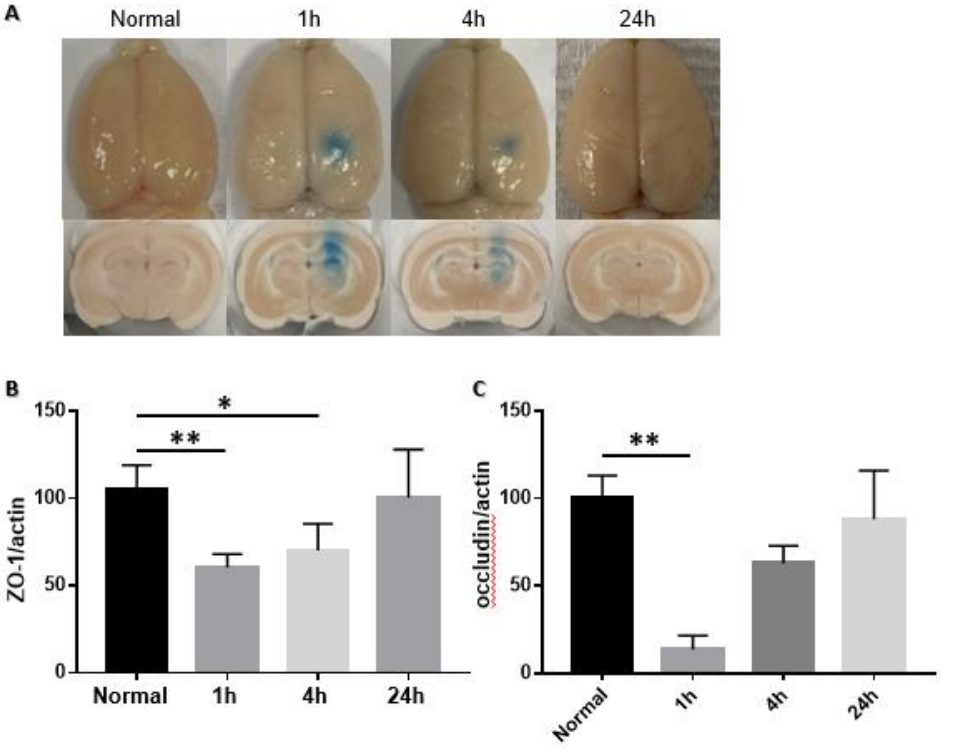

Figure 4. Comparison of Evans blue extravasation and tight junction proteins between the control and FUS groups. (A: Evans blue extravasation in the brain tissue. B,C: Western blot analysis of ZO-1 and Occludin. Data are expressed as mean ± SEM. n = 6 for each group. *P < 0.05, **P < 0.01; parametric analysis was performed using the unpaired t-test)

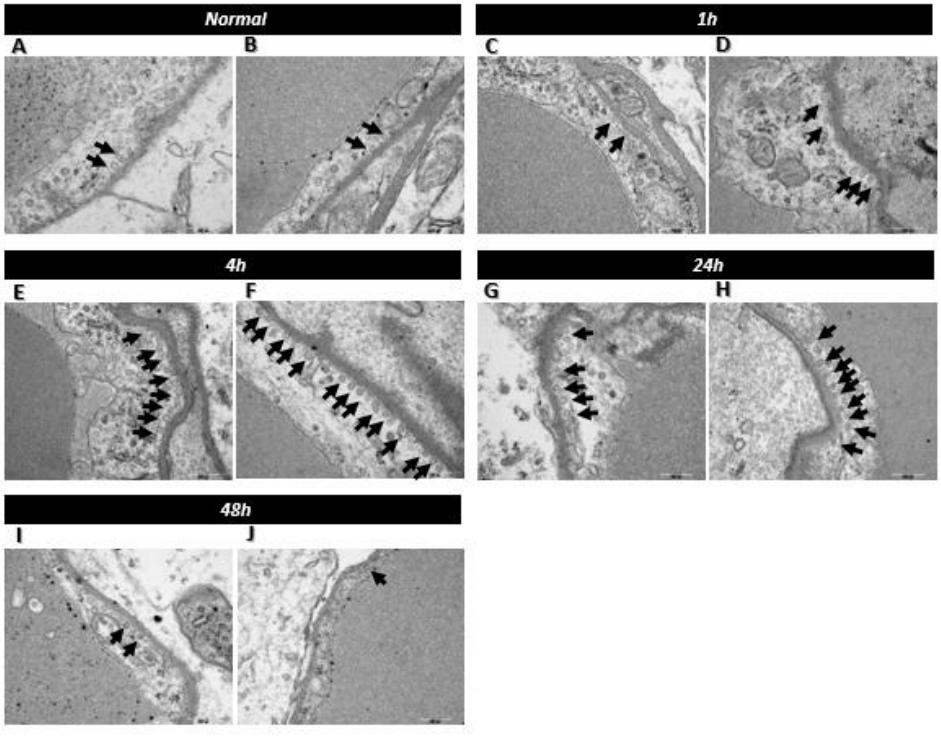

Figure 5. Electron-microscopic examination was used to observe caveolae formation in focused ultrasound treated rats. (Arrow indicates caveolae, A,B: normal, C,D: 1h after sonication, E,F: 4h after sonication, G,H: 24h after sonication, I,J: 48h after sonication, Magnification: 80K, Scale bar, 500 nm)

4. Changes in MFSD2a and caveolin-1 levels after FUS

Western blot analysis was conducted compare the protein levels of MFSD2a and caveolin-1 between control and FUS groups. Mfsd2a levels decreased after FUS. The lowest levels of MFSD2a were observed at 4 h after FUS, whereas caveolin-1 levels peaked at 4 h post-FUS (Figure 6).

5. Expression of caveolin-1 and Reca1 after FUS

Immunohistochemical analysis was performed to examine caveolin-1 and Reca1 (an endothelial cell marker) expression. Expression of caveolin-1 and Reca1 was higher in FUS-treated rats than in untreated rats. Immunohistochemical analysis revealed co-localization of caveolin-1 and Reca1 in the same endothelial cells in the FUS-treated rats (Figure 7).

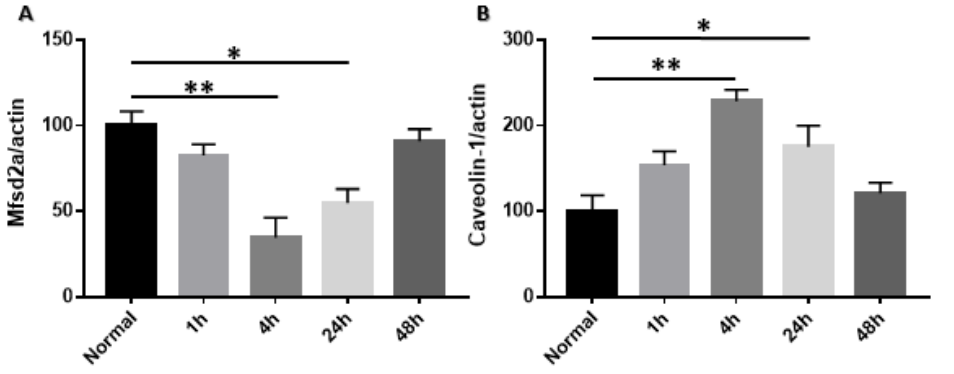

Figure 6. Comparison of mfsd2a and caveolin-1 between the control and FUS groups using Western blot analysis. A: mfsd2a, B: caveolin-1, Data are expressed as mean ± SEM. n = 6 for each group. *P < 0.05, **P < 0.01; parametric analysis was performed using the unpaired t-test

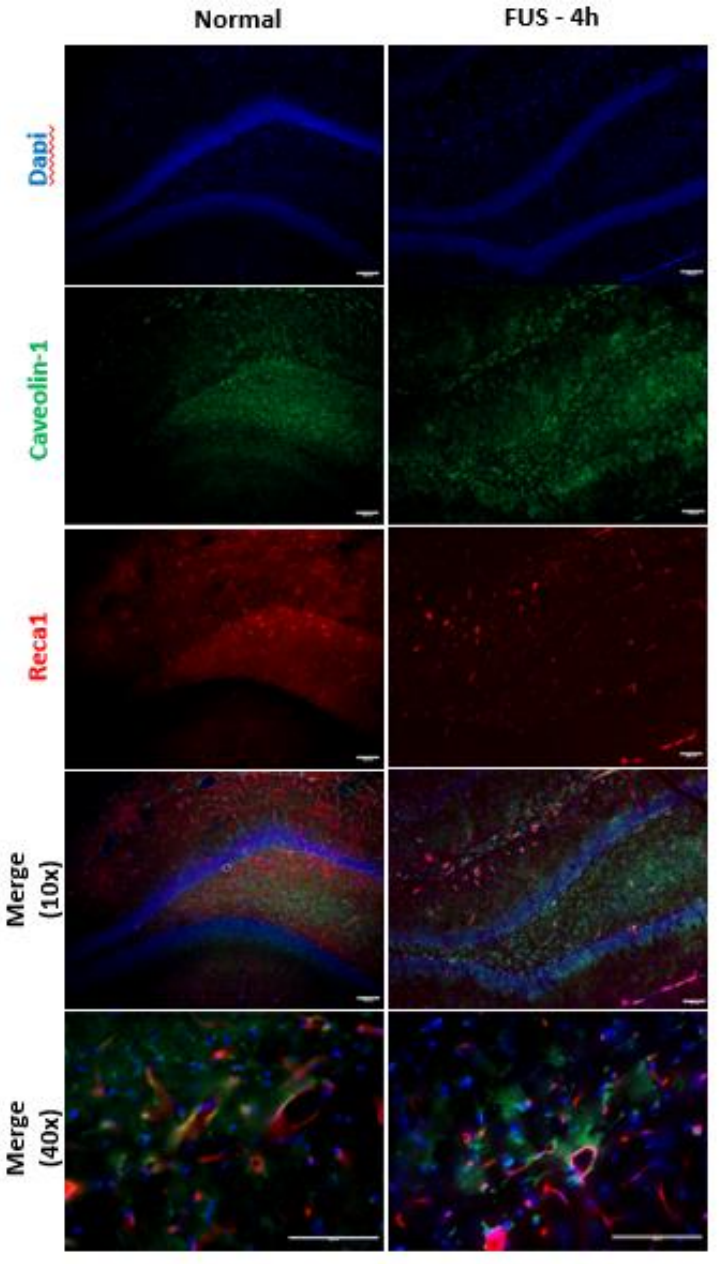

Figure 7. Immunohistochemical analysis of Caveolin-1 and Reca1. Expression of both Caveolin-1 and Reca1 was higher in FUS-treated rats than in untreated rats. Co-localization of Caveolin-1 and Reca1. Scale bar, 100 μm.

IV. DISCUSSION

The use of minimally invasive and reversible BBB opening using low-intensity FUS is an active area of research. However, most studies have reported clinical results obtained by sonication, and the underlying mechanisms of this method are unclear[14,28]. As such, there is an urgent need to elucidate the cellular and molecular mechanisms of low-intensity FUS-mediated BBB opening[18] in order to maximize BBB opening using this approach. Increasing the effectiveness of low-intensity FUS for BBB opening may enhance CNS drug delivery strategies[6,9,29] and clearance of neurotoxic molecules[30,31], and may be expanded to other research fields such as stem cell treatment or genetics[32] in the future.

FUS has the potential to temporarily and reversibly open the BBB with minimal invasiveness. BBB permeability is restored to baseline within 6 to 24 h, with resolution mostly complete by 24 h post-sonication[35]. Moreover, FUS parameters are associated with both the safety and duration of BBB opening. Nevertheless, FUS parameters must be appropriately controlled to minimize adverse effects such as hemorrhage or massive extravasation[33,34]. Additionally, the dose, size, and type of microbubbles can have a significant impact on BBB permeability. Therefore, there have been substantial efforts to identify the optimal FUS parameters for BBB opening, although there is substantial heterogeneity in the parameters recommended by different research groups. This study adopted the parameters used in previous research by our institute's laboratory which proved safety[28].

A proposed mechanism for BBB opening is sheer stress in endothelial cells caused by microbubbles[25], which induce inertial cavitation[36] and result in an acute inflammatory response[37,38]. These events result in transient opening of the BBB and an increase in proteins associated with tight junction stability such as claudin-5, occludin, and ZO-1. Another pathway involved in BBB regulation is vesicle-mediated transportation[39]. Transcytosis permits the entry

of regulated macromolecules such as transferrin and insulin, which are essential for brain function[40]. Caveolae are small membrane invaginations (50-100 nm in diameter) in the plasma membrane which are enriched in cholesterol, glycosphingolipids, and lipid-anchoring proteins[39]. Caveolae are associated with the transcellular transport of macromolecules such as albumin and lipoproteins[41]. Major scaffolding proteins, Caveolins-1, -2 and -3, are associated with these invaginations[40]. Caveolin-1 is a critical early modulator that precedes disruption of tight junctions and the BBB; indeed increased caveolin-1 expression is associated with reduced BBB integrity[42,43]. Ultrasound predominantly affects caveolin-mediated endocytosis rather than clathrin-mediated endocytosis, highlighting the crucial role of caveolae in BBB regulation[21]. In addition, studies have reported increased caveolin-1 expression in animals and *in vitro* models following ultrasound treatment[20,21]. Another study reported that low-intensity FUS resulted in an increase in caveolin-1 protein and caveolin-mediated transcytosis was involved in the transportation of larger cargoes[40].

MFSD2a is a transmembrane protein selectively expressed in vascular endothelial cells[44]. MFSD2a is thought to be associated with changes in lipid composition and caveolae-vesicle formation in endothelial cells[45]. MFSD2a plays a role in transporting docosahexaenoic acid (DHA) into the brain[46] via endothelial cells and maintaining BBB integrity by inhibiting the formation of caveolae in the BBB[47]. In *Mfsd2a* knock-out mice, BBB permeability and brain endothelial cell vesicular transcytosis are increased, but tight junctions are unaffected.[47] Previous studies have demonstrated that MFSD2a may inhibit vesicular transcytosis during BBB injury after intracranial hemorrhage[47,48]. Further, a decrease in MFSD2a contributes to increased vesicular transport in the BBB[48]. However, no studies to date have examined the role of MFSD2a using a BBB opening model. To the best of our knowledge, this is the first study to demonstrate a decrease in MFSD2a levels

after low-intensity FUS-induced BBB opening in an *in vivo* rat model.

Our immunohistochemical and western blot analyses revealed upregulation of caveolin proteins after FUS, indicating that FUS induced active transport of molecules across the BBB. The reduction in levels of tight junction proteins supports the view that molecules moved paracellularly across the BBB following FUS. Tight junction proteins were most prominently downregulated at 1 h following FUS, started to recover after 4 h, and returned to pre-treatment levels at 48 h post-FUS. Levels of caveolin-1 and MFSD2a, which are associated with transcytosis, showed the greatest changes at 4 h post-FUS and recovered to baseline levels at 48 h. Therefore, the results estimate that FUS induced the tight junction breakdown and sequentially enhanced the caveolin mediated transcytosis pathway via downregulating the MFSD2a (Figure 8).

A novel and distinct finding of our study is that there was a time gap between paracellular pathway activity and transcytosis pathway. Although previous studies have demonstrated the two pathways and via downregulation of tight junction proteins and upregulation of Caveolin-1 after FUS, the experimental design of Caveolin-1 didn't focus on the specific time point of each pathway[17,20,21,40]. The study mainly focused on the most permeable BBB time after FUS by Evans blue or MRI, that represents the sum of BBB permeability which can't distinguish the most permeable time of each pathway. After the establishment of the most permeable BBB time point, they performed western blot at the time point to evaluate the caveolin-1 level. However, in this study the experiment was designed to specify the groups in each time point after FUS. Therefore, it was possible to measure the changes in tight junction protein levels or Caveolin-1/MFSd2a levels to distinguish the two pathways. This study has shown that paracellular pathway activity began earlier (1 h post-FUS), followed by transcytosis at 4 h post-FUS. This result is concordant with a previous study that employed two-photon fluorescence

microscopy to evaluate BBB opening. The study demonstrated temporal dynamics of ‘fast or slow’ leakage, with ‘fast’ leakage reaching extracellular peak intensity during FUS treatment and ‘slow’ leakage beginning 5-15 min after FUS treatment and occurring along the vessel length[49]. The authors suggested that ‘fast’ and ‘slow’ leakage corresponded to paracellular and transcellular transport, respectively[49].

The time gap between the two pathways will inform drug delivery strategies, whereby transport of molecules via transcytosis may be more efficient at 4 h after BBB opening, whereas transport via the paracellular pathway may be more efficient at 1 h after sonication. Therefore, pharmacologic delivery of larger, lipophilic and smaller, hydrophilic molecules may be more efficient at 4 h and 1 h after sonication, respectively. Nevertheless, future studies should compare drug delivery times for specific pharmacologic agents. Further, given that the major components of the BBB include endothelial cells of blood vessels and CNS astrocytes, studies examining the role of astrocytes in BBB opening are warranted.

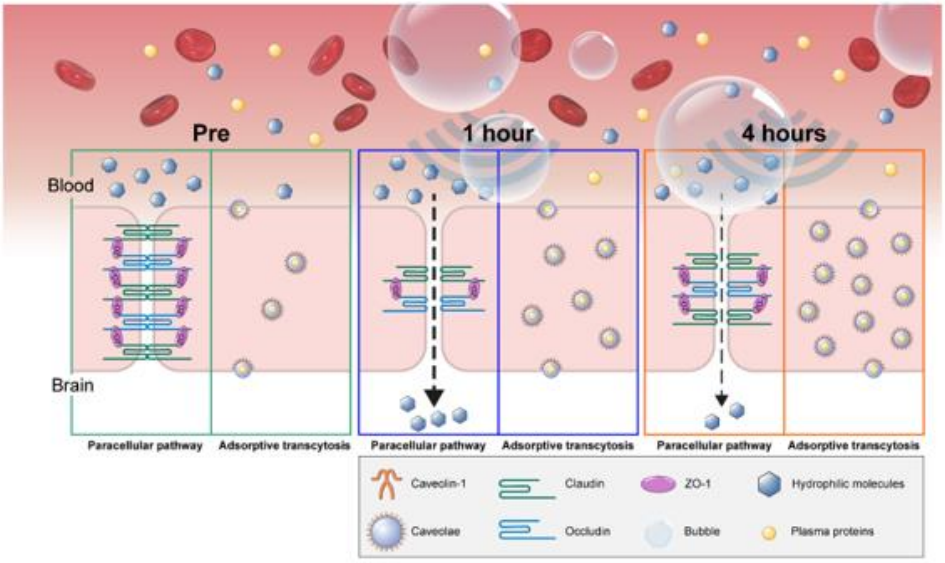

Figure 8. Diagrammatic summary of the study

V. CONCLUSION

FUS is a non-invasive and safe way to open the BBB. Here, in this study demonstrate a time gap between transcytosis and tight junction mechanisms and highlight the molecular mechanisms underscoring FUS-mediated BBB opening. Our findings indicate that different injection times should be adopted when administering drugs following FUS-induced BBB, depending on the specific characteristics of the drug being delivered.

REFERENCES

1. Daneman R, Prat A. The blood-brain barrier. Cold Spring Harb Perspect Biol. 2015;7(1):a020412.
2. Abbott NJ, Ronnback L, Hansson E. Astrocyte-endothelial interactions at the blood-brain barrier. Nat Rev Neurosci. 2006;7(1):41-53.
3. Pardridge WM. CSF, blood-brain barrier, and brain drug delivery. Expert Opin Drug Deliv. 2016;13(7):963-75.
4. Pardridge WM. The blood-brain barrier: bottleneck in brain drug development. NeuroRx. 2005;2(1):3-14.
5. Saitou M, Furuse M, Sasaki H, Schulzke JD, Fromm M, Takano H, et al. Complex phenotype of mice lacking occludin, a component of tight junction strands. Mol Biol Cell. 2000;11(12):4131-42.
6. Burgess A, Shah K, Hough O, Hynynen K. Focused ultrasound-mediated drug delivery through the blood-brain barrier. Expert Rev Neurother. 2015;15(5):477-91.
7. Pandit R, Chen L, Gotz J. The blood-brain barrier: Physiology and strategies for drug delivery. Adv Drug Deliv Rev. 2020;165-166:1-14.
8. Sweeney MD, Zhao Z, Montagne A, Nelson AR, Zlokovic BV. Blood-Brain Barrier: From Physiology to Disease and Back. Physiol Rev. 2019;99(1):21-78.
9. Hersh DS, Wadajkar AS, Roberts N, Perez JG, Connolly NP, Frenkel V, et al. Evolving Drug Delivery Strategies to Overcome the Blood Brain Barrier. Curr Pharm Des. 2016;22(9):1177-93.
10. Obermeier B, Daneman R, Ransohoff RM. Development, maintenance and disruption of the blood-brain barrier. Nat Med. 2013;19(12):1584-96.
11. Zlokovic BV. The blood-brain barrier in health and chronic neurodegenerative disorders. Neuron. 2008;57(2):178-201.
12. Hynynen K, McDannold N, Vykhodtseva N, Jolesz FA. Noninvasive MR imaging-guided focal opening of the blood-brain barrier in rabbits. Radiology. 2001;220(3):640-6.
13. Bakay L, Ballantine HT, Jr., Hueter TF, Sosa D. Ultrasonically produced changes in the blood-brain barrier. AMA Arch Neurol Psychiatry. 1956;76(5):457-67.
14. McDannold N, Arvanitis CD, Vykhodtseva N, Livingstone MS. Temporary disruption of the blood-brain barrier by use of ultrasound and microbubbles: safety

and efficacy evaluation in rhesus macaques. Cancer Res. 2012;72(14):3652-63.

15. Hynynen K. MRI-guided focused ultrasound treatments. Ultrasonics. 2010;50(2):221-9.

16. Hynynen K, McDannold N, Vykhodtseva N, Jolesz FA. Non-invasive opening of BBB by focused ultrasound. Acta Neurochir Suppl. 2003;86:555-8.

17. Sheikov N, McDannold N, Sharma S, Hynynen K. Effect of focused ultrasound applied with an ultrasound contrast agent on the tight junctional integrity of the brain microvascular endothelium. Ultrasound Med Biol. 2008;34(7):1093-104.

18. Sheikov N, McDannold N, Vykhodtseva N, Jolesz F, Hynynen K. Cellular mechanisms of the blood-brain barrier opening induced by ultrasound in presence of microbubbles. Ultrasound Med Biol. 2004;30(7):979-89.

19. Burgess A, Nhan T, Moffatt C, Klibanov AL, Hynynen K. Analysis of focused ultrasound-induced blood-brain barrier permeability in a mouse model of Alzheimer's disease using two-photon microscopy. J Control Release. 2014;192:243-8.

20. Deng J, Huang Q, Wang F, Liu Y, Wang Z, Wang Z, et al. The role of caveolin-1 in blood-brain barrier disruption induced by focused ultrasound combined with microbubbles. J Mol Neurosci. 2012;46(3):677-87.

21. Lionetti V, Fittipaldi A, Agostini S, Giacca M, Recchia FA, Picano E. Enhanced caveolae-mediated endocytosis by diagnostic ultrasound in vitro. Ultrasound Med Biol. 2009;35(1):136-43.

22. Hersh DS, Nguyen BA, Dancy JG, Adapa AR, Winkles JA, Woodworth GF, et al. Pulsed ultrasound expands the extracellular and perivascular spaces of the brain. Brain Res. 2016;1646:543-50.

23. Goertz DE. An overview of the influence of therapeutic ultrasound exposures on the vasculature: high intensity ultrasound and microbubble-mediated bioeffects. Int J Hyperthermia. 2015;31(2):134-44.

24. Nyborg WL. Biological effects of ultrasound: development of safety guidelines. Part II: general review. Ultrasound Med Biol. 2001;27(3):301-33.

25. Chen H, Kreider W, Brayman AA, Bailey MR, Matula TJ. Blood vessel deformations on microsecond time scales by ultrasonic cavitation. Phys Rev Lett. 2011;106(3):034301.

26. Krizanac-Bengez L, Mayberg MR, Janigro D. The cerebral vasculature as a

therapeutic target for neurological disorders and the role of shear stress in vascular homeostatis and pathophysiology. Neurol Res. 2004;26(8):846-53.

27. Boland B, Yu WH, Corti O, Mollereau B, Henriques A, Bezard E, et al. Promoting the clearance of neurotoxic proteins in neurodegenerative disorders of ageing. Nat Rev Drug Discov. 2018;17(9):660-88.
28. Shin J, Kong C, Cho JS, Lee J, Koh CS, Yoon MS, et al. Focused ultrasound-mediated noninvasive blood-brain barrier modulation: preclinical examination of efficacy and safety in various sonication parameters. Neurosurg Focus. 2018;44(2):E15.
29. Chai WY, Chu PC, Tsai MY, Lin YC, Wang JJ, Wei KC, et al. Magnetic-resonance imaging for kinetic analysis of permeability changes during focused ultrasound-induced blood-brain barrier opening and brain drug delivery. J Control Release. 2014;192:1-9.
30. Burgess A, Dubey S, Yeung S, Hough O, Eterman N, Aubert I, et al. Alzheimer disease in a mouse model: MR imaging-guided focused ultrasound targeted to the hippocampus opens the blood-brain barrier and improves pathologic abnormalities and behavior. Radiology. 2014;273(3):736-45.
31. Jordao JF, Thevenot E, Markham-Coultes K, Scarcelli T, Weng YQ, Xhima K, et al. Amyloid-beta plaque reduction, endogenous antibody delivery and glial activation by brain-targeted, transcranial focused ultrasound. Exp Neurol. 2013;248:16-29.
32. McMahon D, Bendayan R, Hynynen K**.** Acute effects of focused ultrasound-induced increases in blood-brain barrier permeability on rat microvascular transcriptome. Sci Rep. 2017;7:45657.
33. Liu HL, Wai YY, Chen WS, Chen JC, Hsu PH, Wu XY, et al. Hemorrhage detection during focused-ultrasound induced blood-brain-barrier opening by using susceptibility-weighted magnetic resonance imaging. Ultrasound Med Biol. 2008;34(4):598-606.
34. Liu HL, Hsu PH, Chu PC, Wai YY, Chen JC, Shen CR, et al. Magnetic resonance imaging enhanced by superparamagnetic iron oxide particles: usefulness for distinguishing between focused ultrasound-induced blood-brain barrier disruption and brain hemorrhage. J Magn Reson Imaging. 2009;29(1):31-8.
35. O'Reilly MA, Hough O, Hynynen K**.** Blood-Brain Barrier Closure Time After

Controlled Ultrasound-Induced Opening Is Independent of Opening Volume. J Ultrasound Med. 2017;36(3):475-83.

36. McDannold N, Vykhodtseva N, Hynynen K. Targeted disruption of the blood-brain barrier with focused ultrasound: association with cavitation activity. Phys Med Biol. 2006;51(4):793-807.

37. Kovacs ZI, Kim S, Jikaria N, Qureshi F, Milo B, Lewis BK, et al. Disrupting the blood-brain barrier by focused ultrasound induces sterile inflammation. Proc Natl Acad Sci U S A. 2017;114(1):E75-E84.

38. McMahon D, Hynynen K. Acute Inflammatory Response Following Increased Blood-Brain Barrier Permeability Induced by Focused Ultrasound is Dependent on Microbubble Dose. Theranostics. 2017;7(16):3989-4000.

39. De Bock M, Van Haver V, Vandenbroucke RE, Decrock E, Wang N, Leybaert L. Into rather unexplored terrain-transcellular transport across the blood-brain barrier. Glia. 2016;64(7):1097-123.

40. Pandit R, Koh WK, Sullivan RKP, Palliyaguru T, Parton RG, Gotz J. Role for caveolin-mediated transcytosis in facilitating transport of large cargoes into the brain via ultrasound. J Control Release. 2020;327:667-75.

41. Pulgar VM. Transcytosis to Cross the Blood Brain Barrier, New Advancements and Challenges. Front Neurosci. 2018;12:1019.

42. Gunzel D, Yu AS. Claudins and the modulation of tight junction permeability. Physiol Rev. 2013;93(2):525-69.

43. Knowland D, Arac A, Sekiguchi KJ, Hsu M, Lutz SE, Perrino J, et al. Stepwise recruitment of transcellular and paracellular pathways underlies blood-brain barrier breakdown in stroke. Neuron. 2014;82(3):603-17.

44. Ben-Zvi A, Lacoste B, Kur E, Andreone BJ, Mayshar Y, Yan H, et al. Mfsd2a is critical for the formation and function of the blood-brain barrier. Nature. 2014;509(7501):507-11.

45. Andreone BJ, Chow BW, Tata A, Lacoste B, Ben-Zvi A, Bullock K, et al. Blood-Brain Barrier Permeability Is Regulated by Lipid Transport-Dependent Suppression of Caveolae-Mediated Transcytosis. Neuron. 2017;94(3):581-94 e5.

46. Nguyen LN, Ma D, Shui G, Wong P, Cazenave-Gassiot A, Zhang X, et al. Mfsd2a is a transporter for the essential omega-3 fatty acid docosahexaenoic acid. Nature.

2014;509(7501):503-6.

47. Yang YR, Xiong XY, Liu J, Wu LR, Zhong Q, Zhou K, et al. Mfsd2a (Major Facilitator Superfamily Domain Containing 2a) Attenuates Intracerebral Hemorrhage-Induced Blood-Brain Barrier Disruption by Inhibiting Vesicular Transcytosis. J Am Heart Assoc. 2017;6(7).
48. Zhao C, Ma J, Wang Z, Li H, Shen H, Li X, et al. Mfsd2a Attenuates Blood-Brain Barrier Disruption After Sub-arachnoid Hemorrhage by Inhibiting Caveolae-Mediated Transcellular Transport in Rats. Transl Stroke Res. 2020;11(5):1012-27.
49. Cho EE, Drazic J, Ganguly M, Stefanovic B, Hynynen K**.** Two-photon fluorescence microscopy study of cerebrovascular dynamics in ultrasound-induced blood-brain barrier opening. J Cereb Blood Flow Metab. 2011;31(9):1852-62.

ABSTRACT(IN KOREAN)

생체 내 쥐 모델에서 저강도 집속 초음파를 이용한 뇌혈관 장벽 개방의 분자생물학적 기전

<지도교수 장 원 석>
연세대학교 대학원 의학과
장 경 원

저강도 집속 초음파는 뇌혈관 장벽을 개방하는데 있어서 새로 각광받고 있는 기술이다. 이러한 방법을 이용한 연구가 많이 되고 있지만 아직까지 정확한 기전을 밝힌 연구가 많지 않다. 이 연구를 통하여 저강도 집속 초음파를 이용한 뇌혈관 장벽의 분자생물학적 기전을 밝히고자 한다. 실험쥐를 이용하여 집속초음파로 뇌혈관 장벽을 개방 후에 무작위로 나뉜 실험군별로 초음파 조사 후 각기 다른 시간점(1시간, 4시간, 24시간, 48시간) 후에 뇌를 추출하여 면역조직화학염색법과 웨스턴블롯 검사를 이용하여 밀착연접 단백질(Occludin과 ZO-1)과 세포내이입에 연관된 단백질 (MFSd2a 와 Caveolin-1)의 양을 측정하였다. 측정 결과 집속 초음파 조사 후 1시간 째에 에반스 블루 염색을 통해 뇌혈관 장벽이 가장 많이 개방되어 있을때 밀착연접 단백질인 Occludin과 ZO-1이 가장 많이 감소하였고, 반면에 Caveolae는 집속 초음파 조사 후 4시간째에 가장 많이 증가하였고 이 시점에 MFSd2a는 가장 많이 감소하였고 Caveolin-1은 가장 많이 증가하였다. 결과를 종합하자면 집속 초음파 후 뇌혈관 개방에는 밀착연접부위의 개방과 세포 내 이입 기전이 모두 연관 되어 있고 두가지 기전에는 시간적 간격이 있었다. 따라서 집속초음파를 이용한 뇌혈관 장벽 개방을 이용한 약물전달 혹은 독성 단백질 제거 등의 임상적 연구 시에 두가지 기전의 시간적 차이를 고려하여 설정하면 도움이 될 것이다.

핵심되는 말 : 뇌혈관 장벽, 집속초음파